



Published in final edited form as:

*Hum Pathol.* 2013 May ; 44(5): 873–880. doi:10.1016/j.humpath.2012.08.013.

## Primary neuroendocrine tumors of the kidney: morphological and molecular alterations of an uncommon malignancy

Phyu P. Aung, MD, PhD<sup>a</sup>, Keith Killian, MD, PhD<sup>b</sup>, Carrie O. Poropatich, MD<sup>c</sup>, W. Marston Linehan, MD<sup>d</sup>, Maria J. Merino, MD<sup>a,\*</sup>

<sup>a</sup>Translational Surgical Pathology, Laboratory of Pathology, National Cancer Institute, National Institutes of Health, Bethesda, MD 20892, USA

<sup>b</sup>Genetics Branch, National Cancer Institute, National Institutes of Health, Bethesda, MD 20892, USA

<sup>c</sup>Department of Pathology, Virginia Hospital Center, Arlington, VA 22205, USA

<sup>d</sup>Urologic Oncology Branch, National Cancer Institute, National Institutes of Health, Bethesda, MD 20892, USA

### Summary

Primary neuroendocrine (NE) tumors of the kidney (PNRTs) are rare and frequently mistaken for other renal and urothelial cancers. We evaluated morphological and molecular findings of 11 PNRTs classified according to the World Health Organization classification of lung NE tumors. Patients included 5 men and 6 women with a median age of 50 years. These tumors occurred in the left (5/11), right (3/11), and horseshoe (1/11) kidney. The histologic patterns were predominantly solid, trabecular, and pseudoglandular. Lymphovascular invasion and calcification were found in 3 and 1 cases, respectively. There were 2 atypical and 9 typical carcinoids. At the time of surgery, 2 patients with atypical carcinoids had hepatic metastasis, and 1 of the typical carcinoid patients had lymph node metastasis. All cases showed <1% proliferative rate, except 2 cases with hepatic metastasis, which showed 3% to 5% with MIB1/Ki-67 immunostaining. Immunostainings were frequently positive for synaptophysin, chromogranin, CD56, CD99, and neuron-specific enolase. Follow-up data (average 4 years) were available for 6 patients. Two patients with distant metastasis were alive with disease, and four patients with no metastasis were alive without disease. We evaluated the association of PNRT and loss of heterozygosity (LOH) on chromosome 3p21 and found LOH in 2 of 3 cases. However, the comparative genomic hybridization study (2/2) did not demonstrate significant chromosomal imbalances. We conclude that PNRTs are positive for NE markers and may have LOH on chromosome 3p21. PNRTs should be classified as NE tumors in other sites, and proliferative rate can be an indicator of aggressive behavior/metastasis.

\*Corresponding author. Laboratory of Pathology, National Cancer Institute (NCI), NIH, Bethesda, MD 20892, USA. mjmerino@mail.nih.gov (M. J. Merino).

## Keywords

Comparative genomic hybridization analysis; Immunohistochemical stain; Loss of heterozygosity analysis; Primary neuroendocrine tumors of the kidney

---

## 1. Introduction

Primary neuroendocrine tumors of the kidney (PNRTs) were first described by Resnick and coworkers in 1966 [1]. Since then, not more than 100 cases have been reported in the literature [2]. The cellular origin of these malignancies remains unclear. It is possible that tumor cells may originate from unrecognized or entrapped neural crest cells in the metanephros during embryogenesis, from neuroendocrine (NE) differentiation of primitive totipotent stem cells, preexisting NE cell hyperplasia from metaplastic/teratomatous epithelium, or that they arise in association with other congenital renal abnormalities such as horseshoe kidney [3-6] and polycystic kidney disease [7-11]. The histologic features of PNRTs are similar to those of NE tumors found at other anatomic locations [12]. Only a few PNRT cases have been analyzed by a limited method of molecular analysis [6,13,14], and the underlying mechanisms of the association with other abnormalities are still not well understood [3-5,7,8,10,15-20].

Hansel et al published a study on 21 PNRTs, stating that this neoplasm occurs in patients with an average age of 52 years and equal gender distribution [14]. Although patients may present with regional lymph node or distant organ metastases, they usually follow a prolonged clinical course [14]. PNRT tumors are frequently unrecognized because they are unusual and have morphologic features that resemble other renal lesions. In this study, we examined 11 cases of PNRTs to further elucidate the morphological and molecular findings associated with these tumors.

## 2. Material and methods

### 2.1. Morphology and immunophenotypic studies

Eleven cases of primary renal neuroendocrine tumors were obtained from the files of the National Cancer Institute between 2001 and 2011. All clinical records as well as pathology materials were available for review. The tumors were classified according to the World Health Organization (WHO) classification of lung NE tumors [21]: well differentiated (typical carcinoid), well differentiated (atypical carcinoid), and poorly differentiated (large/small cell carcinoma). This classification is based mainly on mitotic activity. Tumor with fewer than 2 mitosis per 2 mm<sup>2</sup> or 10 HPF (high-power fields) and lacking necrosis is categorized as a typical carcinoid, and tumor with 2–10 mitosis per 2 mm<sup>2</sup> or 10 HPF and/or foci of necrosis is classified as atypical carcinoid. The poorly differentiated tumors are subclassified into small and large cell NE tumors. Both of them have a mitotic rate >10 per 10HPF and almost always with necrosis. These poorly differentiated tumors are subclassified depending on the size of tumor cells. The small cells are usually less than 3× diameter of a lymphocyte, and cytoplasm is very scant compared to large cell neuroendocrine tumor.

Hematoxylin and eosin–stained slides were reviewed in all cases by two pathologists (P.P.A. and M.J.M.). Representative blocks from each case were selected for immunohistochemical studies using antibodies against CD56 (neural cell adhesion molecule), synaptophysin, chromogranin, inhibin, glucagon, somatostatin, insulin, pancreatic polypeptide, gastrin, neuron-specific enolase (NSE), p53, cytokeratin 7, renal cell carcinoma marker, CD10 (common acute lymphocytic leukemia antigen), CD99 (MIC2), MIB1 (antibody against the Ki-67 antigen), Wilms tumor protein (WT1), epithelial membrane antigen (EMA), vimentin, myogenin, pankeratin, leukocyte common antigen (LCA), cytokeratin 20, and thyroid transcription factor (TTF1). Immunohistochemical results were interpreted as negative or positive.

The percentage of reactive nuclei (MIB1 labeling index) was calculated as the estimated number of positive cells divided by the estimated number of total cells multiplied by 100.

## 2.2. Genetic studies

Loss of heterozygosity (LOH) analysis of the 3p12-3p21 region, using polymerase chain reaction (PCR), was performed in 3 cases. Polymerase chain reaction amplification was performed utilizing the specific markers D3S1560, D3S1597, D3S1317, D3S1038, and D3S1110. Tumor and corresponding normal kidney tissues were manually microdissected under direct light microscope visualization. Briefly, unstained formalin-fixed, paraffin-embedded 5- $\mu$ m-thick tissue sections were prepared on glass slides, deparaffinized, and air dried. One section was stained with hematoxylin and eosin. Tumor and normal cells were selected from each air-dried slide and microdissected using a disposable, 30-gauge needle.

Procured cells were immediately resuspended in a 20 mL solution containing 50 mmol Tris (pH 8.5), 1 mmol EDTA (pH 8.0), 0.5% Tween (Sigma, St. Louis, MO), and 10 mg/ mL proteinase K (pH 8.0) and incubated for 72 hours at 60°C. The mixture was then boiled for 5 min to inactivate proteinase K, and 1.5 L of this solution was used for PCR analysis. Tumor and normal DNA from each case was subjected to heating for 9 min at 95°C followed by 35 cycles of PCR under the following conditions: 60°C for 2 min, 94°C for 1 min, followed by an extension step of 1 cycle at 72°C for 5 min.

PCR was performed in 10 L reactions containing 1 L 10 $\times$  PCR buffer (100 mM Tris–HCl, pH 8.3 [at 25°C]; 500 mmol KCl; 15 mmol MgCl<sub>2</sub>; 0.01% gelatin); 0.8 L each of 20 mM deoxycytidine triphosphate, deoxyguanosine triphosphate, deoxythymidine triphosphate, and deoxyadenosine triphosphate; 5.6 L millipore water; 0.4 L of 50 pM of each primer; 0.2 L [<sup>32</sup>P] deoxycytidine triphosphate (6000 Ci/mmol/L); and 0.1 U of *Taq* DNA polymerase (AmpliTaq Gold, 250 U, 5 U/mL; Perkin Elmer, Norwalk, CT). Labeled amplified DNA was mixed with an equal volume of formamide sample buffer (238 mL formamide, 0.25% bromophenol blue, 0.25% xylene cyanol, and 12 mmol EDTA pH 8.0). The samples were denatured for 5 min at 94°C and loaded onto a 6% acrylamide gel. Samples were electrophoresed at 1800 V for 2 hours, and gels were transferred to 3-mm Whatman paper and dried for 1 h at 80°C, and autoradiography was performed with Kodak X-OMAT film (Eastman Kodak, Rochester, NY). A locus was considered informative for a particular patient when the constitutional DNA from that patient displayed two different alleles (heterozygous at that locus), and LOH was present when one of the 2 polymorphic alleles

present in the normal tissue DNA was absent or reduced in the tumoral DNA by at least 60%.

Comparative genomic hybridization (CGH) was also done to evaluate the presence of genetic gains or losses in two of three PNRT cases that were also studied for LOH analysis. Tumor DNA was extracted under histological guidance from formalin-fixed paraffin-embedded tissue blocks. Extracted DNA was profiled for chromosomal aberrations using Agilent 4×180K oligonucleotide arrays (Agilent Inc, Santa Clara, CA), and image data were analyzed with Nexus 5.0 software (Nexus, Okland, CA) using standard settings. CGH plots were visually analyzed for regions of gross chromosomal aberration.

### 3. Results

#### 3.1. Demographic and clinical findings

Patient demographics are summarized in Table 1. Briefly, patients ranged in age from 35 to 65 years, with an average age of 50 years. There were 5 males and 6 females. The tumors in most patients were detected accidentally (80%), whereas 20% of the patients presented with signs or symptoms associated with the tumor, including back or flank pain, hematuria, enlarging abdominal mass, anemia, and weight loss. None of these patients had clinical signs or symptoms of carcinoid syndrome or familial history of renal or other cancers. In one patient, the tumor occurred in a horseshoe kidney.

Two patients underwent radical nephrectomy with lymph node dissection, and nine patients underwent partial nephrectomy. Laterality was left in 5 of 11 cases (53%), right in 3 of 11 (47%), a horseshoe kidney in one case, and unknown in 2 patients. No other tumor masses were clinically or radiographically identified in the majority of patients, which was consistent with a primary renal tumor. At the time of initial surgery, distant metastasis to the liver was seen in 2 patients, and 1 patient had metastatic disease to a regional lymph node.

#### 3.2. Pathologic findings

All of the tumors were single mass ( $n = 11/11$ ) affecting different areas including the upper pole ( $n = 4/8$ ), lower pole ( $n = 3/8$ ), and renal pelvis ( $n = 1/8$ ). Location was unknown in 3 cases. Tumor size ranged from 3.2 to 11 cm (average, 7.1 cm). The two atypical carcinoids with hepatic metastasis were 10 and 11 cm, whereas one typical carcinoid with lymph node metastasis was 5.2 cm. The tumors were classified based on the mitotic figures according to the WHO classification of NE tumors of lungs. All tumors were well-differentiated carcinoids, 9 (82%) typical and 2 (18%) atypical, with 3 and 5 mitosis per 10 HPF, respectively. There were no poorly differentiated neuroendocrine (small/ large cell) carcinomas.

Most of the cases showed clear demarcation between tumor and adjacent renal parenchyma ( $n = 9/11$ ; 82%). The two remaining cases, which had hepatic metastasis, revealed microinfiltration into the surrounding renal parenchyma, and lymphovascular invasion was found in the cases with distant metastasis. The predominant histologic patterns of tumor consisted of trabecular with ribbon-like appearance (Fig. 1A), solid (Fig. 1B), and pseudoglandular. NE tumors are mainly composed of uniform polygonal cells with scant to

moderate amount of eosinophilic cytoplasm, round to elongated nuclei with salt and pepper chromatin, and inconspicuous nucleoli. Small focal calcifications were present in 1 of 11 cases (9%) (Fig. 2). Most tumors demonstrated 0–2 mitoses/10HPF (9/11), although a few demonstrated up to 5 mitoses/10HPF (2/11). None of the cases exhibited areas of necrosis.

### 3.3. Immunohistochemical findings

The results of immunohistochemical stains are summarized in Table 2. Synaptophysin was the most commonly positive marker (n = 11/11; Fig. 1C). In addition, expression of chromogranin (8/11), CD56 (5/5), CD 99 (1/1), NSE (1/1), CD10 (1/2), vimentin (1/1; focally), inhibin (1/1; weakly), and pankeratin (1/3; weakly and focally) was detected. Immunostains for TTF-1 (n = 2), glucagon (n = 2), somatostatin (n = 1), insulin (n = 4), gastrin (n = 2), pancreatic polypeptide (n = 2), p53 (n = 1), WT1 (n = 4), EMA (n = 2), vimentin (n = 1), myogenin (n = 1), LCA (n = 1), cytokeratin 7 (n = 4), cytokeratin 20 (n = 4), TTF1 (n = 2), renal cell marker (n = 1), and S100 (n = 1) were negative. MIB1 immunostaining was available in five cases; staining of tumor cells (<2%) was seen in 3 cases, which included the one with lymph node metastasis, and 3% and 5% staining (Fig. 1D) were seen in 2 cases with distant metastasis to liver.

### 3.4. Genetic findings

We performed microdissection and DNA extraction in tumor and respective normal renal parenchyma of three cases for LOH analysis of the 3p12-3p21. Two of three cases (67%) showed LOH on chromosome 3p21 (Fig. 3) similar to a clear cell renal carcinoma. CGH was done in two of these three cases to evaluate the presence of genetic gains or losses, but no significant chromosomal imbalances were detected (Fig. 4).

### 3.5. Clinical outcome

Clinical followed up data were obtained for 6 patients, ranging from 2 to 6 years (average, 4 years). One patient had metastatic disease to a local para-aortic lymph node (n = 1/11). Four of the 6 patients (67%) are still alive with no evidence of recurrent/residual disease. Two of the patients (33%), with distant metastasis to the liver, are still alive with disease.

## 4. Discussion

The pathogenesis of renal neuroendocrine tumors is still unknown. Guy et al reported that no neuroendocrine cells were detected in kidneys of children and fetuses and could not validate the hypothesis that the origin of neuroendocrine tumor cells is entrapped/misplaced progenitor cells during organogenesis [16].

Primary neuroendocrine tumors of the kidney are rare and frequently misdiagnosed with other kidney and urothelial cancers such as papillary type 1 renal cell carcinoma, mesonephric tumors, Wilms tumor, or undifferentiated carcinoma. Although PNRTs demonstrated the relatively characteristic appearance of typical carcinoid tumors, a high occurrence of misdiagnosis was found in the submitted cases of our study, most probably due to the uncommonness of this disease. We found that most of the misdiagnoses were caused by the morphologic similarities of primitive neuroendocrine tumor to other renal

malignancies, lack of suspicion for this entity, and insufficient ancillary studies such as immunostainings.

The patients in our study were evenly divided between men and women. Renal carcinoid tumor appeared to present at a younger age than usual renal cell carcinoma, with many patients in our study presenting at approximately 50 years of age as previously reported [14,22]. One patient had a horseshoe kidney from which the renal carcinoid appeared to arise, which was similar to prior reports [18,22]. One study reported that 73.6% of the tumors >4 cm had metastases [22]. The majority of our cases were <5 cm in tumor size (8/11). The only exceptions were tumors from the patients with distant metastasis (2/11), which were 10 and 11 cm in size, and one tumor with a lymph node metastasis (1/11), which was 5.2 cm in size.

Prior studies demonstrated that the most common clinical presentation of PNRT was tumor-related symptoms, commonly flank/back pain [22]. However, the NE tumors in most of our patients (80%) were discovered incidentally on workup for other conditions. In our study, most of the tumors (9/ 11) demonstrated very low metastatic rate with prolonged survival. None of the patients had distant metastatic disease at the time of initial diagnosis. Previous reports have documented the development of metastatic disease in patients with renal carcinoid tumor [14,17,19,23-25]. A few studies have correlated poor patient outcomes with increased mitotic activity and cytologic atypia within the renal carcinoid tumor [14,26]. Similar to the previous findings, in our study, although most of the cases demonstrated low mitotic rates, ranging from 0 to 2 per 10 HPF, the 2 cases with hepatic metastasis demonstrated the highest mitotic rate (3-5 mitoses/10 HPF).

Immunohistochemical stainings were consistent with the diagnosis of neuroendocrine tumor, with the majority of cases demonstrating strong immunoreactivity for synaptophysin, chromogranin, CD56, and NSE. In addition, CD99 positive expression was seen in one of the cases examined, which supports the previous finding that CD99 expression was seen in almost all cases of renal carcinoid [27]. This CD99 positivity made it more difficult to differentiate this rare tumor from primitive neuroendocrine tumors. One of the main differential diagnoses of PNRTs is type 1 papillary renal cell carcinoma especially with a compact tubulopapillary histologic pattern. In PNRT, absence of papillary architecture with fibrovascular core frequently with foamy histiocytes and negative expression of cytokeratin 7 immunostain are helpful to differentiate from type 1 papillary renal cell carcinoma. Moreover, absence of WT 1 immunostain in PNRT can exclude other morphologic differential diagnoses, adult Wilms tumor and nephrogenic rests. Paraganglioma, one of the differential diagnoses, is differentiated by the absence of S100 positive sustentacular cells. Cytokeratin 7, cytokeratin 20, TTF 1, and LCA were negative in all cases studied, ruling out a gastrointestinal/ lung metastasis or lymphoma. In addition, the loss of staining by gastrin, somatostatin, glucagon, insulin, and pancreatic polypeptide also excludes metastatic neuroendocrine tumors from the gastrointestinal tract. Neuroendocrine phenotype was supported by the focal staining of vimentin in one examined case. Negative staining for CD56 and positive staining for CD57 and pankeratin of mesonephric tumors may be helpful to differentiate them from this rare entity.

Molecularly analyzed data in PNRT are limited. Two previous reports have documented a loss of heterozygosity at the D3F15S2 locus of 3p21 in one case [6]. In our study, LOH of the 3p12-3p21 region was found in 2 of 3 cases, suggesting a possible common genetic event in the molecular genesis of PNRT tumors as in the most common renal cell carcinoma, clear cell type. No specific genetic gains or losses were identified in the CGH study, which may be explained by lack of specificity of the technique.

In conclusion, this study reports 11 well differentiated primary renal carcinoid tumors. This neoplasm often occurs in patients around 50 years of age, affects male and female patients with equal frequency, and appears to present with tumor-related symptoms. Morphologically, PNRT is consistent with carcinoid tumors present at other anatomic sites. A small percentage of these patients may present with regional lymph node metastases or distant organ metastases but usually have a prolonged clinical course despite distant metastatic disease. None of the tumors <5 cm or 2 mitosis/ 10 HPF reveal distant metastasis. One of the renal PNRTs arose from a horseshoe kidney. The tumors are positive for neuroendocrine markers and may have LOH on chromosome 3p21 similar to a clear cell renal carcinoma. No significant chromosomal imbalances were found in the CGH study. In this rare primary neuroendocrine tumor of kidney, the WHO classification of NE tumor used in other organs should be used, and a high proliferative rate is an indicator of aggressive behavior or metastasis of these tumors.

## References

- [1]. Resnick ME, Unterberger H, McLoughlin PT. Renal carcinoid producing the carcinoid syndrome. *Med Times* 1966;94:895–6. [PubMed: 5938842]
- [2]. Canacci AM, MacLennan GT. Carcinoid tumor of the kidney. *J Urol* 2008;180:2193. [PubMed: 18804792]
- [3]. Begin LR, Guy L, Jacobson SA, Aprikian AG. Renal carcinoid and horseshoe kidney: a frequent association of two rare entities—a case report and review of the literature. *J Surg Oncol* 1998;68:113–9. [PubMed: 9624041]
- [4]. Faucompret S, Farthouat P, Deligne E, Louis C, Breda Y. Kidney cancer in horseshoe kidney. A case report of an unexpected diagnosis. *Ann Urol (Paris)* 2002;36:81–6. [PubMed: 11969053]
- [5]. Rodríguez-Covarrubias F, Gómez X, Valerio JC, Lome-Maldonado C, Gabilondo F. Carcinoid tumor arising in a horseshoe kidney. *Int Urol Nephrol* 2007;39:373–6. [PubMed: 16835722]
- [6]. van den Berg E, Gouw AS, Oosterhuis JW, et al. Carcinoid in a horseshoe kidney. Morphology, immunohistochemistry, and cytogenetics. *Cancer Genet Cytogenet* 1995;84:95–8. [PubMed: 8536229]
- [7]. Fetissov F, Benatre A, Dubois MP, Lanson Y, Arbeille-Brassart B, Jobard P. Carcinoid tumor occurring in a teratoid malformation of the kidney. An immunohistochemical study. *Cancer* 1984;54:2305–8. [PubMed: 6386141]
- [8]. Kojiro M, Ohishi H, Isobe H. Carcinoid tumor occurring in cystic teratoma of the kidney: a case report. *Cancer* 1976;38:1636–40. [PubMed: 991082]
- [9]. Shibata R, Okita H, Shimoda M, et al. Primary carcinoid tumor in a polycystic kidney. *Pathol Int* 2003;53:317–22. [PubMed: 12713568]
- [10]. Soulié M, Escourrou G, Vazzoler N, et al. Primary carcinoid tumor and horseshoe kidney: potential association. *Prog Urol* 2001;11:301–3. [PubMed: 11400494]
- [11]. Yoo J, Park S, Jung LH, Jin KS, Kee KB. Primary carcinoid tumor arising in a mature teratoma of the kidney: a case report and review of the literature. *Arch Pathol Lab Med* 2002;126:979–81. [PubMed: 12171501]

- [12]. World Health Organization Classification of Tumors In: Eble JN, Sauter G, Epstein JI, Sesterhenn IA, editors. Pathology and genetics of tumours of the urinary system and male genital organs. Lyon, France: IARC Press; 2004 p. 138.
- [13]. el-Naggar AK, Troncso P, Ordonez NG. Primary renal carcinoid tumor with molecular abnormality characteristic of conventional renal cell neoplasms. *Diagn Mol Pathol* 1995;4:48–53. [PubMed: 7735556]
- [14]. Hansel DE, Epstein JI, Berbescu E, Fine SW, Young RH, Cheville JC. Renal carcinoid tumor: a clinicopathologic study of 21 cases. *Am J Surg Pathol* 2007;31:1539–44. [PubMed: 17895755]
- [15]. Buntley D. Malignancy associated with horseshoe kidney. *Urology* 1976;8:146–8. [PubMed: 960345]
- [16]. Guy L, Bégin LR, Oligny LL, Brock GB, Chevalier S, Aprikian AG. Searching for an intrinsic neuroendocrine cell in the kidney. An immunohistochemical study of the fetal, infantile and adult kidney. *Pathol Res Pract* 1999;195:25–30. [PubMed: 10048091]
- [17]. Isobe H, Takashima H, Higashi N, et al. Primary carcinoid tumor in a horseshoe kidney. *Int J Urol* 2000;7:184–8. [PubMed: 10830826]
- [18]. Krishnan B, Truong LD, Saleh G, Sirbasku DM, Slawin KM. Horseshoe kidney is associated with an increased relative risk of primary renal carcinoid tumor. *J Urol* 1997;157:2059–66. [PubMed: 9146580]
- [19]. McVey RJ, Banerjee SS, Eyden BP, Reeve RS, Harris M. Carcinoid tumor originating in a horseshoe kidney. *In Vivo* 2002;16:197–9. [PubMed: 12182116]
- [20]. Unger PD, Russell A, Thung SN, Gordon RE. Primary renal carcinoid. *Arch Pathol Lab Med* 1990;114:68–71. [PubMed: 2403781]
- [21]. World Health Organization classification of tumours In: Travis WD, Brambilla E, Muller-Hermelink HK, Harris CC, editors. Pathology and Genetics of Tumours of the Lung, Pleura, Thymus and Heart. Lyon, France: IARC Press; 2004 p. 19–20.
- [22]. Romero FR, Rais-Bahrami S, Permpongkosol S, Fine SW, Kohanim S, Jarrett TW. Primary carcinoid tumors of the kidney. *J Urol* 2006;176:2359–66. [PubMed: 17085102]
- [23]. Cauley JE, Almagro UA, Jacobs SC. Primary renal carcinoid tumor. *Urology* 1988;32:564–6. [PubMed: 3201667]
- [24]. Raslan WF, Ro JY, Ordonez NG, et al. Primary carcinoid of the kidney. Immunohistochemical and ultrastructural studies of five patients. *Cancer* 1993;72:2660–6. [PubMed: 8402487]
- [25]. Tal R, Lask DM, Livne PM. Metastatic renal carcinoid: case report and review of the literature. *Urology* 2003;61:838. [PubMed: 12670585]
- [26]. Takeshima Y, Inai K, Yoneda K. Primary carcinoid tumor of the kidney with special reference to its histogenesis. *Pathol Int* 1996;46:894–900. [PubMed: 8970200]
- [27]. Jeung JA, Cao D, Selli BW, et al. Primary renal carcinoid tumors: clinicopathologic features of 9 cases with emphasis on novel immunohistochemical findings. *Hum Pathol* 2011;42:1554–61. [PubMed: 21496872]



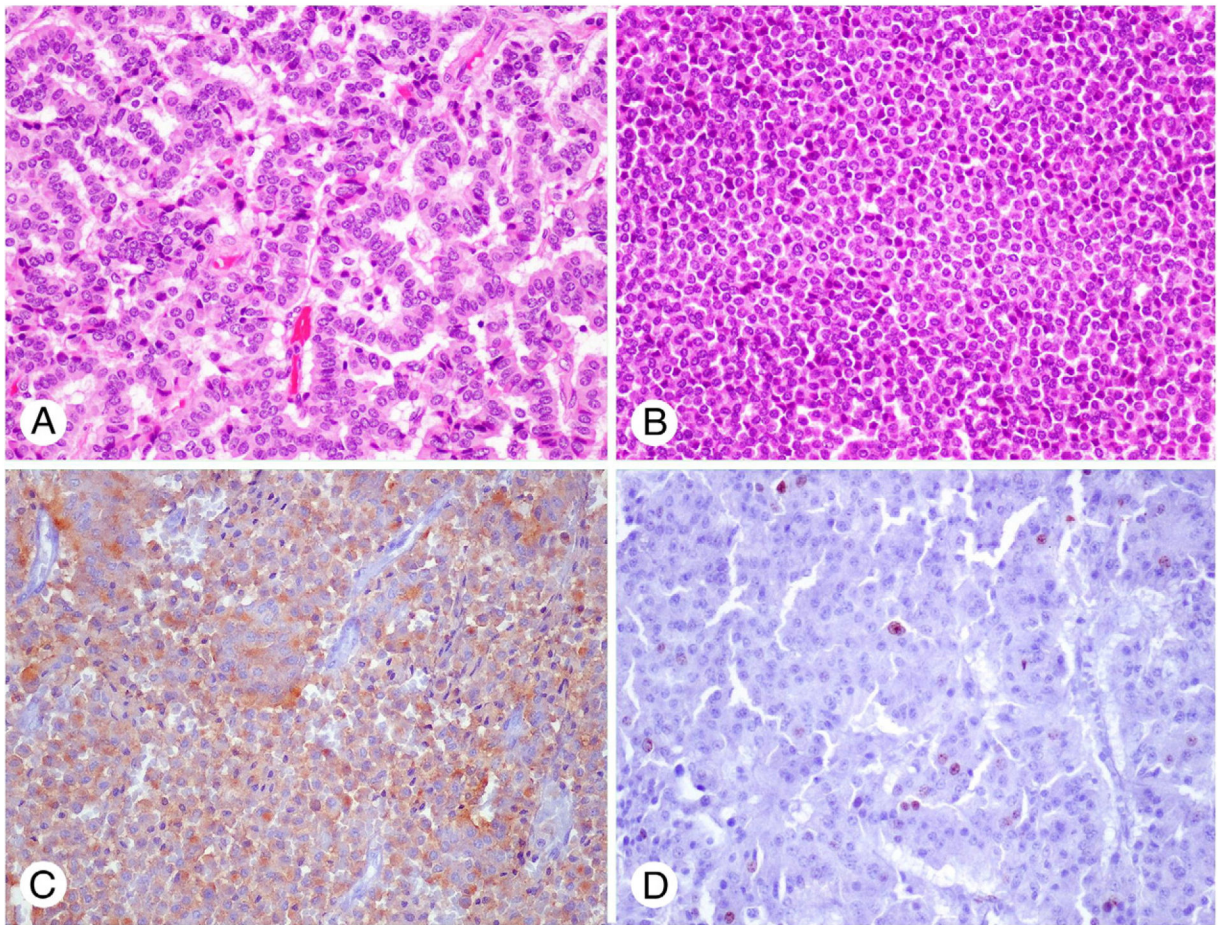


**Fig. 1.** Representative figure (H&E) of primary neuroendocrine tumor of kidney: PNRT with trabecular appearance (A) and solid (B). Synaptophysin (C) and MIB1 (D) in a PNRT with liver metastasis and high mitotic index (5%) (A-D: original magnification  $\times 20$ ). Abbreviation: H&E, hematoxylin and eosin.

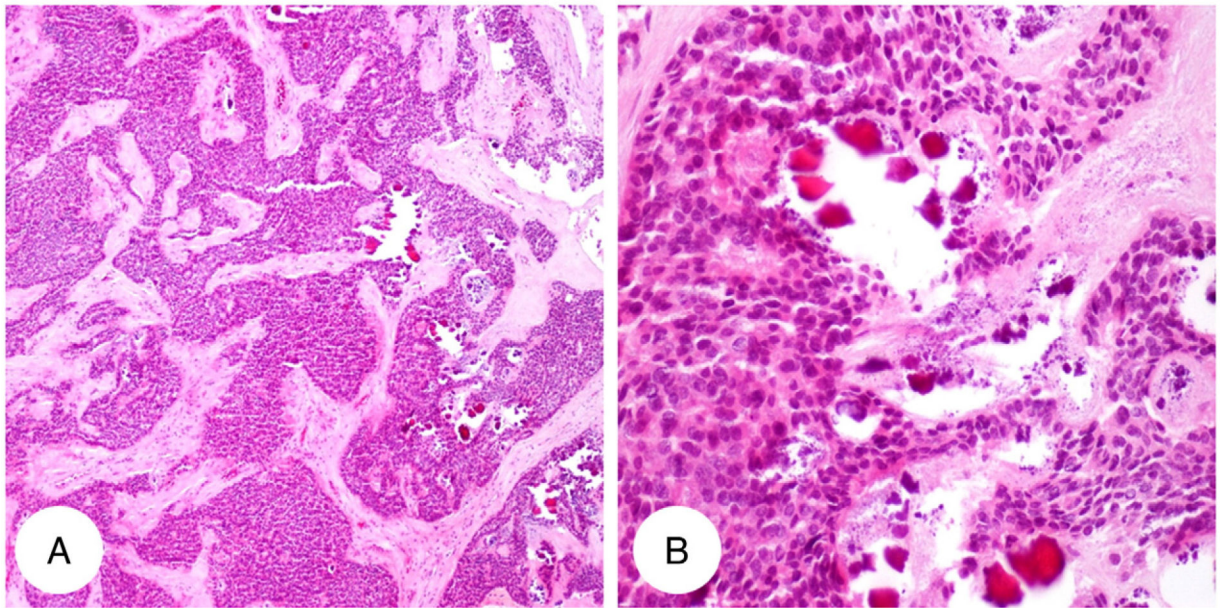


**Fig. 2.**  
Representative figure of focal calcification in primary neuroendocrine tumor of kidney (H&E; A: original magnification  $\times 4$ ; B: original magnification  $\times 20$ ).

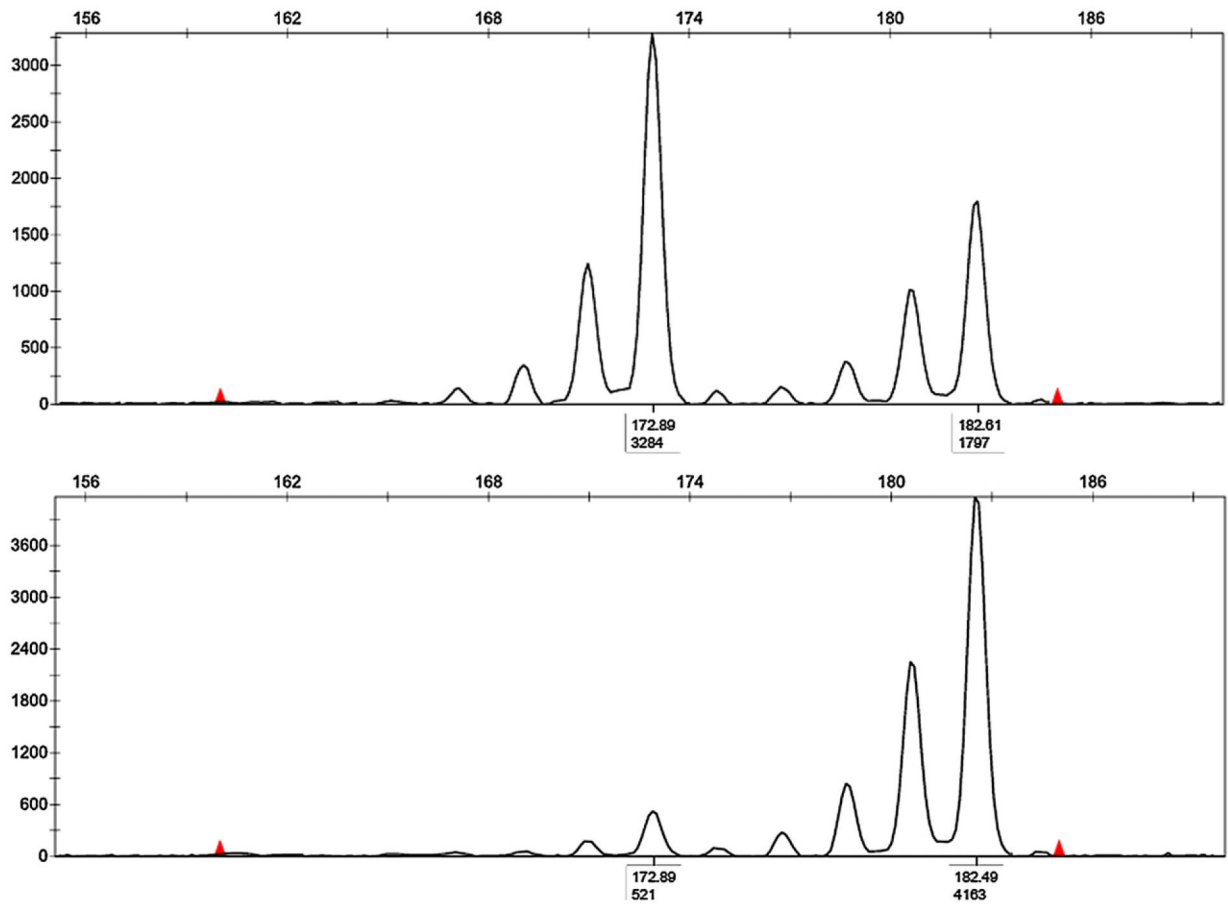


**Fig. 3.**

Representative figure of semi-automated assessment of LOH using the D3S1597 marker. The peak heights in fluorescent units are shown on the Y-axis on the left. A, Amplification from normal adjacent renal parenchyma cells demonstrating two alleles. B, An example of a complete allele deletion (LOH) in tumor cells from the same patient. Tumor cells demonstrate only the second allele. LOH was calculated by comparison of the allele ratio of normal cells with the allele ratio in tumor cells (521/3284). The criterion for LOH was at least a 60% reduction of the lesional allele, with the subsequent modification of the allele ratio.

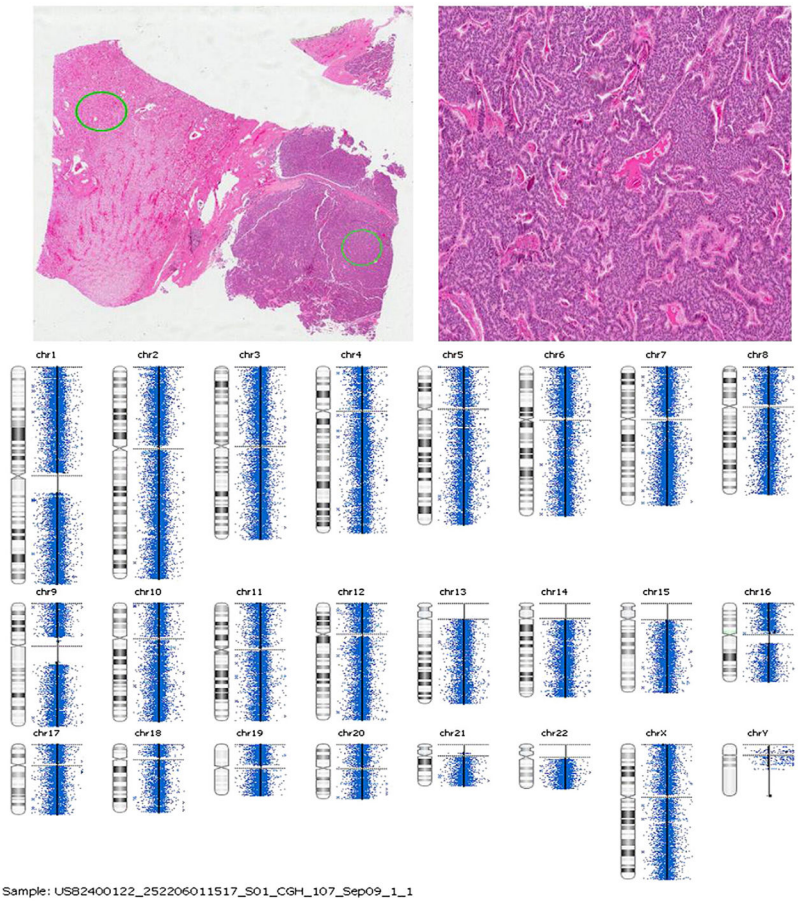


**Fig. 4.**  
Representative figure of CGH array analysis.

**Table 1**

## Patient demographic information

<b>Clinicopathologic features</b>	<b>Findings</b>
Patient age (y), range (mean)	35-65 (50)
Clinical presentation	11/11
Incidental	8/11
Abdominal mass	2/11
Flank/back pain	3/11
Hematuria	2/11
Anemia	1/11
Weight loss	1/11
Laterality	9/11
Left	5/11
Right	3/11
Horseshoe	1/11
Location	8/11
Upper pole	4/8
Lower pole	3/8
Renal pelvis	1/8
Metastasis at surgery	3/11
Lymph node	1/11
Liver	2/11
Patient with clinical follow up	6/11
Alive with disease	2/11
Alive without disease	4/11
Sex (M/F)	5:6
Tumor size (cm)	3.2-11

**Table 2**

## Summary of immunohistochemical findings

IHC stains	Positive	Negative
Chromogranin	8/11	3/11
Synpatophysin	11/11	0
CD56	5/5	
CD99	1/1	
NSE	1/1	
Inhibin	1/1 (weak)	
Glucagon		2/2
Somatostatin		1/1
Insulin		4/4
Gastrin		2/2
Pancreatic polypeptide		2/2
P53		1/1
WT1		4/4
EMA		2/2
Vimentin	1/1 (focal)	
Myogenin		1/1
Pankeratin	1/3 (weak &focal)	2/3
LCA		1/1
CK7		4/4
CK20		4/4
TTF1		2/2
CD10	1/2	1/2
Renal cell marker		1/1
S100		1/1
MIB1		
2%	3/5	
5%	2/5	